Theoretical prediction of atomic and electronic structure of neutral Si_6O_m (m=1–11) clusters

María C. Caputo, Ofelia Oña,[a] and Marta B. Ferraro[b]
Departamento de Física, Facultad de Ciencias Exactas y Naturales, Universidad de Buenos Aires, Ciudad Universitaria, Pab. I (1428) Buenos Aires, Argentina

(Received 14 October 2008; accepted 20 January 2009; published online 7 April 2009)

In this paper we found the most stable structures of silicon-oxide clusters of Si_6O_m (m=1–11) by using the genetic algorithm. In this work the genetic algorithm uses a semiempirical energy function, MSINDO, to find the best cluster structures of Si_6O_m (m=1–11). The best structures found were further optimized using the density functional theory. We report the stable geometries, binding energies, lowest unoccupied molecular orbital-highest occupied molecular orbital gap, dissociation energies for the most favorable fragmentation channels and polarizabilities of Si_6O_m (m=1–11). For most of the clusters studied here we report structures not previously found using limited search approaches on common structural motifs. © *2009 American Institute of Physics*.
[DOI: 10.1063/1.3080549]

I. INTRODUCTION

Silica is a very important material, one of the most abundant materials on earth.[1] Its nanoparticles are interesting because of their importance in technological applications, such as microelectronics[2] and optics,[3] its uses, ranging from glass to catalysis,[4] and the very important optical fiber communications.[5] Since silica is one of the materials that shows novel properties in the nanoscale range, the study and understanding of the structure, bonding, stability, and properties of their clusters and nanoparticles is very important and necessary.[6] Since El-Shall and co-workers[7] observed bright blue photoluminescence in silica, different authors tried to justify the experimental observation by large concentration of oxygen defects related to the size of the lowest unoccupied molecular orbital-highest occupied molecular orbital (LUMO-HOMO) gap.[8] Silica clusters show light absorption[8] and photoluminescence[9] because their particular structures are very different from the conventional bulk material. Another interest is silica as a molecular building material, since the combination of its bulk stability and the advantage of its abundance put it in a very good position to be exploited via synthetic methods.[10]

Cages and tubes of SiO_2 are an integral constituent part of the extended periodic systems known as zeolites.[11] Silicon oxides have a fundamental role in the growth of SiNWs because it has been proven experimentally that the yield of SiNWs will be greatly enhanced if silicon oxide is present during the synthesis.[12]

The structure and properties of silicon oxides clusters have been studied from both experimental[13–16] and theoretical points of view.[17–19] Photoelectron spectra of some silicon oxide anions have been studied by Wang *et al.*,[14–16] providing information about electronic structures of the clusters. Chelikowsky[17] found that buckled rings of Si_4O_4 and Si_5O_5 are more stable than planar ones. Song and Choi[20] compared the stability of elongated and compact SiO_2 clusters with 12–46 molecules using plane-wave density-functional theory (DFT) and provided a very good discussion about effects of size, morphology, and different types of silica rings and their electronic and optical properties. Nayak *et al.*[21] studied structure and properties of $(SiO_2)_n$ (n=1–6) and Si_3O_n (n=1,3,4) employing *ab initio* methodology, while Zhang *et al.*[19] and Chu *et al.*[22] provided a detailed theoretical study of structures of Si_nO_m (n,m=1–8) by the DFT-B3LYP (Ref. 23) method. Zhang *et al.*[24] demonstrated that the two- (2MR) and three-membered ring (3MR) hybrid clusters are energetically more favorable than the pure 2MR or 3MR clusters indicating their suitability like blocks of construction for new materials.

Wang *et al.*[25] studied the segregation of Si_nO_n in different motifs because of the great interest in the observation of high-yield silicon nanowire (SiNW) growth from SiO vapor.[12,26,27] Experiments showed that SiNWs can be obtained by thermal evaporation or laser ablation of Si powder mixed with SiO_2 or SiO,[12,26,27] but there is no SiNWs growth from pure SiO_2 materials.[12] Reber *et al.*[28] demonstrated that SiO units assemble to form bigger clusters, with silicon rich agglomerations at the center and oxygen rich structures at the periphery.

In spite of the large number of calculations of properties and electronic of oxide clusters, the understanding of their structures is still an open subject. In this article we propose to search for the structures of Si_6O_m in the energy hypersurface employing our modified genetic algorithms (MGAC) package,[29–31] which uses the parallel implementation of genetic algorithms (PGA),[31] a stochastic method. PGA is, in conjunction with basin-hopping Monte Carlo[32,33] and simulated annealing,[34] one of the best approaches to explore and find global and secondary minima of complex energy potential surfaces. This simulation technique permits to handle

[a]Author to whom correspondence should be addressed. Electronic mail: ofelia@df.uba.ar.
[b]Member of Carrera del Investigador de CONICET.

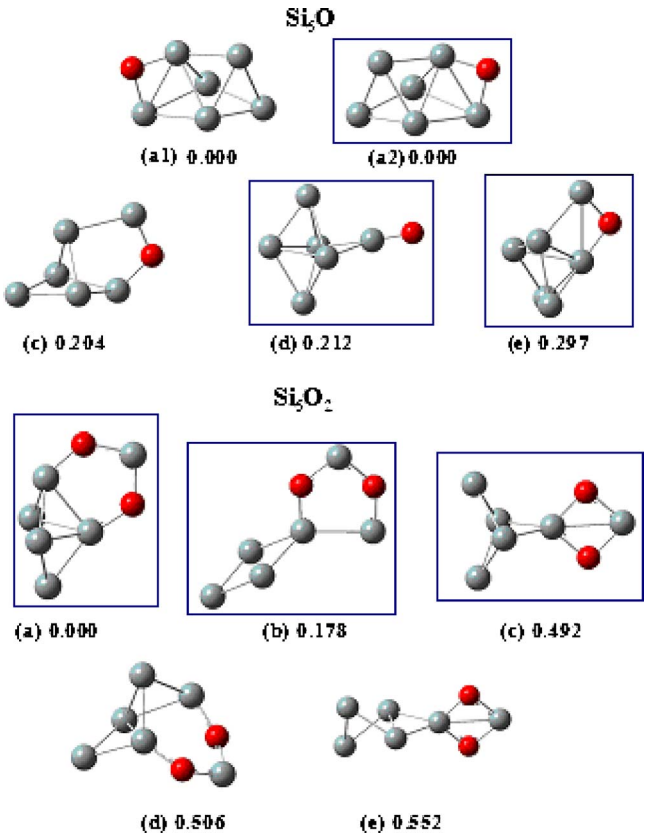

FIG. 1. (Color online) Optimized structures for the five lower-energy isomers for Si_6O and Si_6O_2 clusters at the B3LYP/6-311G(2*d*) level of theory. BE in eV based on a Si atomic energy of −7847.211 eV and O atomic energy of −2036.020 eV. The structures similar to those reported in the literature are enclosed by frames.

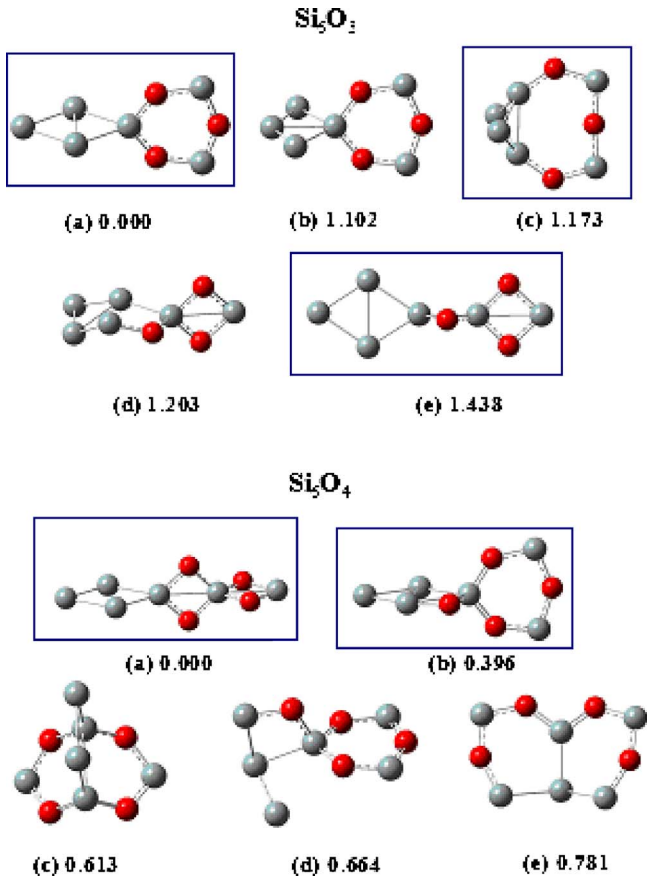

FIG. 2. (Color online) Optimized structures for the five lower-energy isomers for Si_6O_3 and Si_6O_4 clusters at the B3LYP/6-311G(2*d*) level of theory. BE in eV based on a Si atomic energy of −7847.211 eV and O atomic energy of −2036.020 eV. The structures similar to those reported in the literature are enclosed by frames.

with clusters of large size. It is not forthcoming to determine isomers of more than ten atoms with traditional methodology, such as DFT, *ab initio*, *etc.* PGA provides not only the global minima, but also other isomers close to the minima.

Current computational limitations make it unfeasible to use *ab initio* or DFT methods in extensive genetic algorithms (GA) searches, therefore we adopted the same recipe that proved to be successful in silicon clusters prediction.[30,35] We use a semiempirical molecular orbital program, MSINDO,[36–38] to evaluate the energy of the clusters in the global search using the GA, while a DFT method to refine those more promising ones by performing a local optimization of the best structures found by the GA. This global search assures that Si_6O_m isomers are produced from a full exploration of the MSINDO/DFT potential energy, without the limitations of DFT relaxed structures obtained by adding *m* oxygen atoms, one by one, to different Si_6 isomers. In an attempt to understand better the electronic properties in the formation of these clusters,[39,40] we studied two series: (i) Si_6O_m ($m=2,3,4,5,6$), which can be thought as small Si_n clusters plus small oxide fragments and (ii) Si_6O_m ($m=9,10,11$), clusters rich in oxygen, which show that the more stable ones are those for which the silicon atoms are more coordinated to oxygen ones.

II. METHODOLOGY

In order to determine the most stable isomers, a stochastic method which uses PGA has been used. Bazterra *et al.*[31] implemented the MGAC package using parallel techniques. The coding method used here allows making it very portable as well as easy to maintain and upgrade. The cluster is represented by a genome of dimension 3*N*, where *N* is the number of atoms in the cluster. Moreover, any genetic operator, mating, crossover, mutation, etc., applied to this genome produces a valid individual, i.e., a possible structure for the desired cluster size. The GA operations of mating, crossover, and also the "cut and slice" operator introduced by Johnston and Roberts[41] are used to evolve one generation into the next one. The best individuals among the population, 50% in our case, are directly copied into the next generation, and the other 50% is replaced applying the genetic operators. This technique is also known as elitism. The criteria for fitness probability, selection of the individuals, and genetic operators are discussed in detail in Ref. 29. GA procedure was run several times to guarantee that the resulting structures are independent of the initial population and statistically significant. We ran the MGAC about five times per Si_6O_m system, employing from 60 to 200 generations with 60 individuals. All the energy calculations were done with the MSINDO code.[36–38] The isomers selected by MGAC/MSINDO calculations were fully optimized using the DFT method with B3LYP exchange correlation functional, employing 6-311G(2*d*) basis sets. Vibration frequencies were calculated for the optimized structures to check that no imaginary fre-

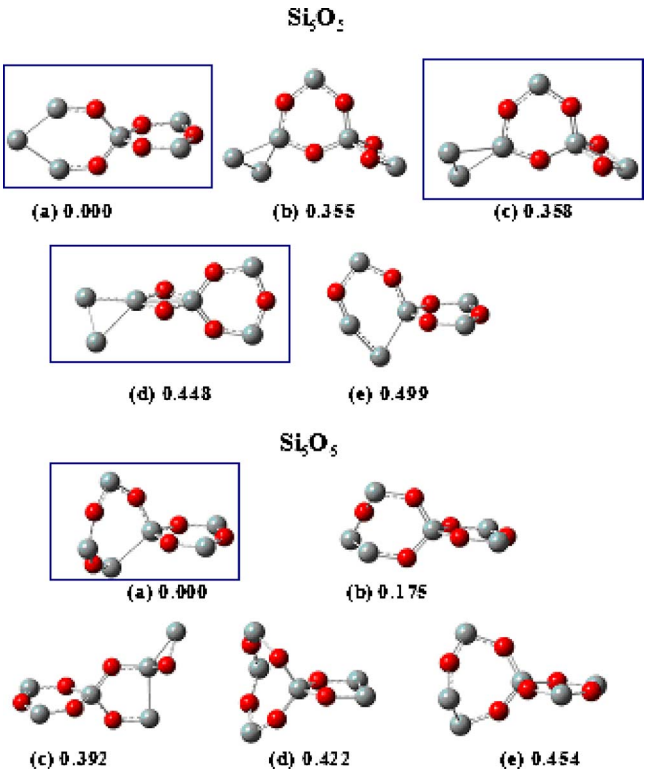

FIG. 3. (Color online) Optimized structures for the five lower-energy isomers for Si_6O_5 and Si_6O_6 clusters at the B3LYP/6-311G(2*d*) level of theory. BE in eV based on a Si atomic energy of −7847.211 eV and O atomic energy of −2036.020 eV. The structures similar to those reported in the literature are enclosed by frames.

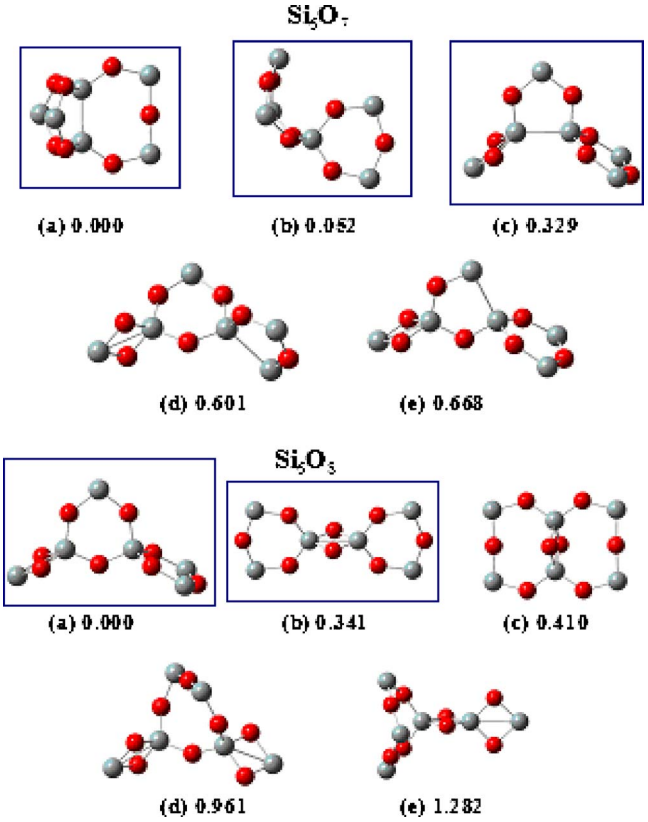

FIG. 4. (Color online) Optimized structures for the five lower-energy isomers for Si_6O_7 and Si_6O_8 clusters at the B3LYP/6-311G(2*d*) level of theory. BE in eV based on a Si atomic energy of −7847.211 eV and O atomic energy of −2036.020 eV. The structures similar to those reported in the literature are enclosed by frames.

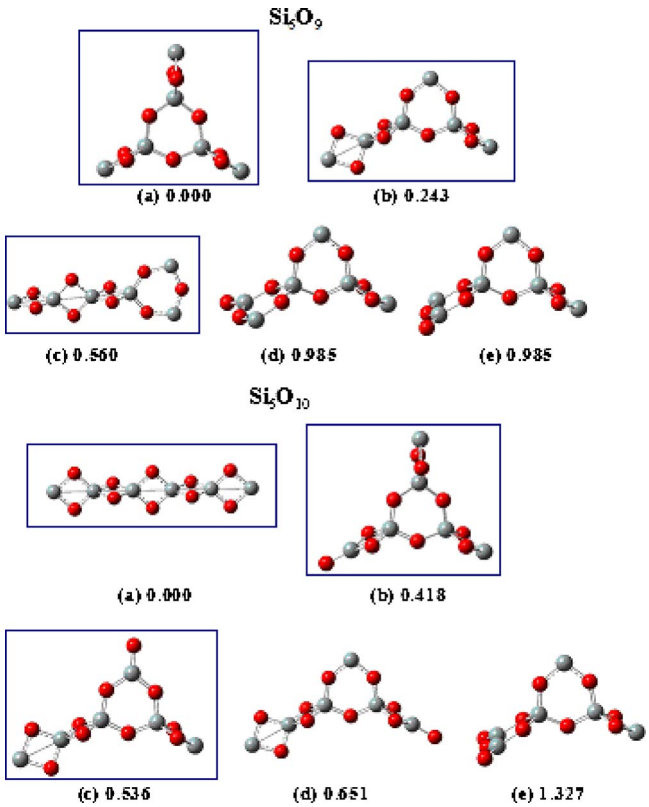

FIG. 5. (Color online) Optimized structures for the five lower-energy isomers for Si_6O_9 and Si_6O_{10} clusters at the B3LYP/6-311G(2*d*) level of theory. BE in eV based on a Si atomic energy of −7847.211 eV and O atomic energy of −2036.020 eV. The structures similar to those reported in the literature are enclosed by frames.

quencies are present. All these calculations were done using the package of programs GAUSSIAN 98.[42]

III. RESULTS AND DISCUSSION

Figures 1–6 show the stable structures of the five lowest-energy isomers for Si_6O_m ($m=1-11$) clusters obtained by the MGAC/MSINDO prediction and followed by the

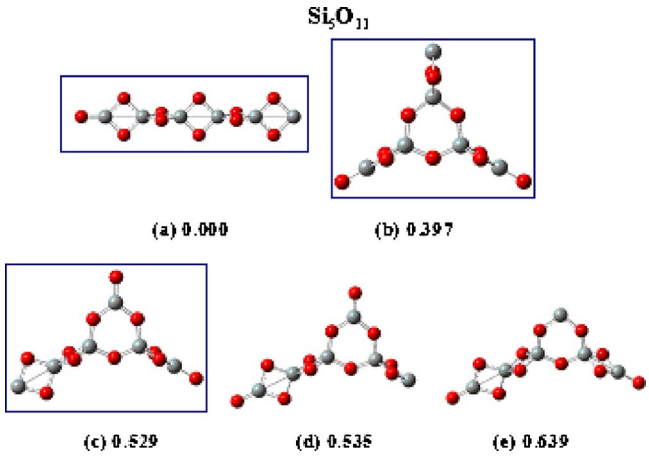

FIG. 6. (Color online) Optimized structures for the five lower-energy isomers for Si_6O_{11} clusters at the B3LYP/6-311G(2*d*) level of theory. BE in eV based on a Si atomic energy of −7847.211 eV and O atomic energy of −2036.020 eV. The structures similar to those reported in the literature are enclosed by frames.

TABLE I. rms between this work and the work of Chelikowsky (Ref. 17) 2MR, 3MRS, and Si_3O_2 reported by Wang *et al.* (Ref. 14) geometry parameters, for Si_6O_m (m=2–11) clusters.

		rms				rms	
System	Fragment	Distance (Å)	Angle (deg)	System	Fragment	Distance (Å)	Angle (deg)
Si_6O_2-*a*	Si_3O_2	0.048	3.5	Si_6O_6-*c*	Si_3O_3	0.023	3.3
Si_6O_2-*b*	Si_3O_2	0.020	3.4		Si_3O_2	0.032	4.9
Si_6O_2-*c*	Si_2O_2	0.006	0.4	Si_6O_6-*d*	Si_4O_4	0.020	10.6
Si_6O_2-*e*	Si_2O_2	0.015	0.8		Si_3O_2	0.090	3.3
				Si_6O_6-*e*	Si_3O_3	0.022	3.8
Si_6O_3-*a*	Si_3O_3	0.013	2.5				
Si_6O_3-*b*	Si_3O_3	0.007	2.2	Si_6O_7-*b*	Si_3O_3	0.020	3.5
Si_6O_3-*d*	Si_2O_2	0.022	1.4		Si_4O_4	0.018	9.9
Si_6O_3-*e*	Si_2O_2	0.023	1.3	Si_6O_7-*c*	Si_2O_2	0.020	1.3
					Si_3O_3	0.018	3.3
Si_6O_4-*a*	$Si_2O_{2\text{-first}}$	0.030	2.2		Si_3O_2	0.061	2.8
	$Si_2O_{2\text{-second}}$	0.032	1.9	Si_6O_7-*d*	Si_2O_2	0.027	1.7
Si_6O_4-*b*	Si_3O_3	0.018	3.4		Si_3O_3	0.029	4.1
Si_6O_4-*c*	Si_3O_2	0.028	5.3		Si_3O_2	0.017	3.7
Si_6O_4-*d*	Si_3O_3	0.013	2.6	Si_6O_7-*e*	Si_2O_2	0.029	1.8
					Si_3O_3	0.012	2.8
Si_6O_5-*a*	Si_3O_3	0.025	3.6		Si_3O_2	0.031	5.1
Si_6O_5-*b*	Si_2O_2	0.031	1.9				
	Si_3O_3	0.028	3.5	Si_6O_8-*a*	Si_2O_2	0.028	1.8
Si_6O_5-*c*	Si_2O_2	0.030	1.9		$Si_3O_{3\text{-first}}$	0.036	4.5
	Si_3O_3	0.029	3.2		$Si_3O_{3\text{-second}}$	0.025	3.6
Si_6O_5-*d*	Si_2O_2	0.026	1.8	Si_6O_8-*b*	Si_2O_2	0.035	2.9
	Si_3O_3	0.028	3.7		$Si_3O_{3\text{-first}}$	0.027	3.3
Si_6O_5-*e*	Si_3O_3	0.013	2.5		$Si_3O_{3\text{-second}}$	0.027	3.3
				Si_6O_8-*c*	Si_2O_2	0.032	2.7
Si_6O_6-*a*	Si_3O_3	0.009	2.8	Si_6O_8-*d*	$Si_2O_{2\text{-first}}$	0.028	1.8
Si_6O_6-*b*	Si_3O_3	0.021	3.1		$Si_2O_{2\text{-second}}$	0.027	1.8
	Si_3O_2	0.070	4.2	Si_6O_8-*e*	$Si_2O_{2\text{-first}}$	0.034	2.7
					$Si_2O_{2\text{-second}}$	0.032	1.8
					Si_4O_4	0.024	11.8
Si_6O_9-*a*	$Si_2O_{2\text{-first}}$	0.032	2.0	Si_6O_{10}-*d*	$Si_2O_{2\text{-first}}$	0.035	2.0
	$Si_2O_{2\text{-second}}$	0.032	2.0		$Si_2O_{2\text{-second}}$	0.038	2.7
	$Si_2O_{2\text{-third}}$	0.032	2.0		$Si_2O_{2\text{-third}}$	0.036	2.5
	Si_3O_3	0.046	5.1		Si_3O_3	0.041	4.6
Si_6O_9-*b*	$Si_2O_{2\text{-first}}$	0.037	2.7	Si_6O_{10}-*e*	Si_2O_2	0.033	2.0
	$Si_2O_{2\text{-second}}$	0.032	1.9		$Si_3O_{3\text{-first}}$	0.045	4.3
	$Si_2O_{2\text{-third}}$	0.031	2.2		$Si_3O_{3\text{-second}}$	0.040	4.9
	Si_3O_3	0.038	4.3				
Si_6O_9-*c*	$Si_2O_{2\text{-first}}$	0.038	2.8	Si_6O_{11}-*a*	$Si_2O_{2\text{-first}}$	0.036	2.4
	$Si_2O_{2\text{-second}}$	0.037	2.6		$Si_2O_{2\text{-second}}$	0.040	2.7
	$Si_2O_{2\text{-third}}$	0.034	2.0		$Si_2O_{2\text{-third}}$	0.040	2.7
	Si_3O_3	0.030	3.7		$Si_2O_{2\text{-fourth}}$	0.039	2.7
Si_6O_9-*d*	$Si_3O_{3\text{-first}}$	0.037	4.7		$Si_2O_{2\text{-fifth}}$	0.037	2.1
	$Si_3O_{3\text{-second}}$	0.037	3.9	Si_6O_{11}-*b*	$Si_2O_{2\text{-first}}$	0.036	2.5
	Si_2O_2	0.031	1.8		$Si_2O_{2\text{-second}}$	0.036	2.5
Si_6O_9-*e*	$Si_3O_{3\text{-first}}$	0.037	4.6		$Si_2O_{2\text{-third}}$	0.039	2.3
	$Si_3O_{3\text{-second}}$	0.037	3.9		Si_3O_3	0.049	5.3
	Si_2O_2	0.031	1.9	Si_6O_{11}-*c*	$Si_2O_{2\text{-first}}$	0.038	2.1
					$Si_2O_{2\text{-second}}$	0.039	2.8
Si_6O_{10}-*a*	$Si_2O_{2\text{-first}}$	0.035	2.0		$Si_2O_{2\text{-third}}$	0.037	2.5
	$Si_2O_{2\text{-second}}$	0.038	2.6		Si_3O_3	0.048	4.7
	$Si_2O_{2\text{-third}}$	0.039	2.6	Si_6O_{11}-*d*	$Si_2O_{2\text{-first}}$	0.036	2.4
	$Si_2O_{2\text{-fourth}}$	0.038	2.6		$Si_2O_{2\text{-second}}$	0.040	2.9
	$Si_2O_{2\text{-fifth}}$	0.035	2.0		$Si_2O_{2\text{-third}}$	0.039	2.3
Si_6O_{10}-*b*	$Si_2O_{2\text{-first}}$	0.036	2.5		Si_3O_3	0.047	4.7
	$Si_2O_{2\text{-second}}$	0.035	2.1	Si_6O_{11}-*e*	$Si_2O_{2\text{-first}}$	0.036	2.5
	$Si_2O_{2\text{-third}}$	0.035	2.1		$Si_2O_{2\text{-second}}$	0.040	2.9

TABLE I. (*Continued.*)

System	Fragment	rms Distance (Å)	rms Angle (deg)	System	Fragment	rms Distance (Å)	rms Angle (deg)
	Si_3O_3	0.047	5.2		$Si_2O_{2\text{-third}}$	0.036	2.4
Si_6O_{10}-*c*	$Si_2O_{2\text{-first}}$	0.035	2.0		Si_3O_3	0.042	4.7
	$Si_2O_{2\text{-second}}$	0.035	2.8				
	$Si_2O_{2\text{-third}}$	0.036	2.2				
	Si_3O_3	0.046	4.6				

B3LYP/6-311G(2*d*) scheme for their final local minimization and their corresponding binding energies (BE) per atom, with respect to the most stable structure for each system. Energies in eV are based on a Si atomic energy of −7847.211 eV and an O atomic energy of −2036.020 eV. The isomers enclosed into frames are those that have been previously reported in the literature.[39,40] The ordering of the energies for the Si_6O_m isomers might be different if they are evaluated by MSINDO method because semiempirical methods do not include correlation.

Although we found new structures such as the Si_6O-*a*1 isomer, which is the mirror structure of the Si_6O-*a*2 isomer, in most cases the structures agree with those reported by Zang *et al.*[39] Si-rich clusters have a tendency to form two fragments, one made of pure silicon atoms and the other made of silicon oxides, Si_2O_2 (2MR), Si_3O_3 (3MR), and Si_4O_4 (4MR, 2MR).[40] On the contrary, for O-rich clusters the isomers prefer the hybrid combinations of 2MR and 3MR.

We inform in Table I the rms between the geometrical parameters of our predicted 2MR, 3MR, 4MR, and those reported by Chelikowsky.[17] The rms of bond distances and bond angles are about 0.02 Å and 3°, respectively, in motifs 2MR or 3MR. The greater distortions can be found in the angles, as it happens, for example, for the 3MR present in the system Si_6O_{11}-*b* (5.3°) and for the 2MR of the systems Si_6O_8 and Si_6O_{11}-*d* (2.9°). In both cases, all the oxygen atoms that form the fragment in question show hypervalent bonds. These distortions are smaller than those which run from 9.9° to 11.8° for the 4MR present in Si_6O_6-*d*, Si_6O_7-*b*, and Si_6O_8-*e* clusters. Si-rich clusters, Si_6O_2, Si_6O_4, Si_6O_6, and Si_6O_7, are formed by Si_3O_2 molecules. We include in Table I the rms between the geometrical parameters of this motif and that reported by Wang *et al.*[14] In this case the rms of bond distances and bond angles are about 0.05 Å and 4°. To sum up, we could say that the motif of 2MR and 3MR are the ones that preserve their distances and their angles in the different systems. At the same time we point out that every time that the system counts with the necessary number of oxygen and silicon atoms to form the motifs 2MR and 3MR, these combinations appear in the cluster. This finding was highlighted by Zhang *et al.*,[24] "These 2MR and 3MR hybrid clusters would be considered as energetically favorable structural models of silica nanoclusters."

In Fig. 7, we reported the moment of total inertia per its maximum component in a function of the number of oxygen atoms for the most stable isomer of each cluster. It is observed that the structures are mainly prolate (rugby football, or cigar shaped), except for the isomer Si_6O_7-*a*, which is more compact, and the isomer Si_6O_9-*a*, which is more oblate (saucer or disk-shaped). For $m \geq 4$, we can see that the most stable structures present Si atoms with four-coordination by oxygen atom, except for the systems Si_6O_6 and Si_6O_7, which present three-coordination by oxygen atom and one-

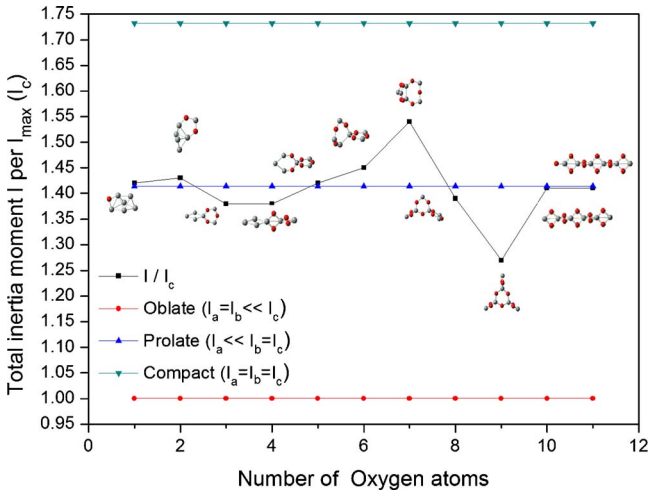

FIG. 7. (Color online) The moment of total inertia I per its maximum component I_c in function of the number m of oxygen atoms for the most stable isomer for each Si_6O_m system.

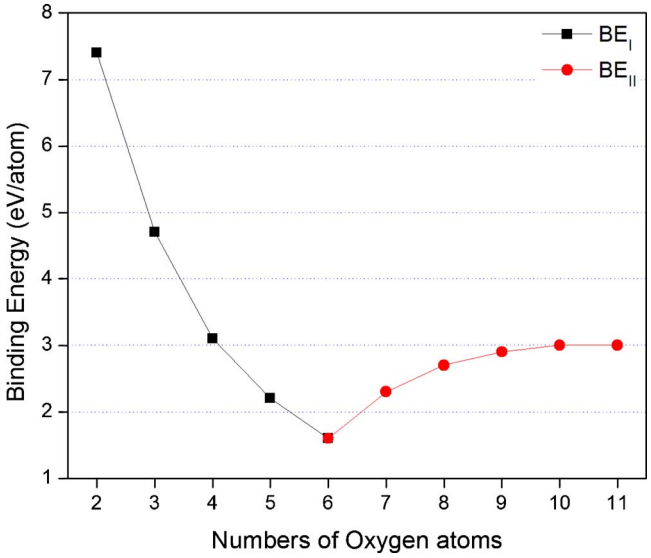

FIG. 8. (Color online) BE per oxygen atom of the lowest-energy isomers for Si_6O_m (m=2–11) clusters [see Eq. (7)].

coordination by silicon atom. For silicon-oxide systems, silicon atoms prefer to form tetrahedral sp^3 hybrid bonds to neighboring oxygen atoms, as it is mentioned by Zhang and Fan[40] We also study the BE/atom for the most stable clusters found in this work as a function of the number of oxygen atoms.

Si_6O_m clusters might be dissociated into silicon oxides, silicon atoms, and oxygen.

$$Si_6O_m \rightarrow aSiO_2 + bSiO + cSi + d\tfrac{1}{2}O_2 \quad (1)$$

requires an energy,

$$BE = E(Si_6O_m) - aE(SiO_2) - bE(SiO) - cE(Si) - d\tfrac{1}{2}E(O_2). \quad (2)$$

We are interested in the preferred dissociation channel, that is, the determination of a, b, c, and d values that, for each m, minimize BE. Conservation of the number of silicon and oxygen atoms requires $a+b+c=6$ and $2a+b+d=m$, respectively. Furthermore, defining the two positive quantities

$$E_x = 2E(SiO_2) + E(Si) - E(SiO), \quad (3)$$

$$E_y = E(SiO) + \tfrac{1}{2}E(O_2) - E(SiO_2), \quad (4)$$

we can rewrite Eq. (2) as

$$BE = Si_6O_m + (6-c)E_x + (m-d)E_y - 6E(Si) - m\tfrac{1}{2}E(O_2). \quad (5)$$

Since E_x and E_y are positive, maximization of BE requires minimization of c and d subject to the b, c, and $d>0$. Our results are

$$m<6 \rightarrow a=0 \;\; b=m \;\; c=6-m \;\; d=0,$$

$$6<m<12 \rightarrow a=m-6 \;\; b=12-m \;\; c=0 \;\; d=0, \quad (6)$$

$$12<m \rightarrow a=6 \;\; b=0 \;\; c=0 \;\; d=m-12.$$

In Fig. 8, we display the tendencies for the proposed dissociation channels for the most stable clusters found in this work as a function of the number of oxygen atoms.

$$BE_I = [E(Si_6O_m) - mE(SiO) - (6-m)E(Si)]/m \quad m \le 6,$$

$$BE_{II} = [E(Si_6O_m) - (m-6)E(SiO_2) - (12-m)E(SiO)]/m \quad 6 < m \le 12, \quad (7)$$

where E is the total energy of the cluster or the atom indicated between brackets. These plots agree with our results above, see Eq. (6). So, it is interesting to note that for Si-rich clusters it is easy to dissociate them into SiO pieces and Si atoms (BE_I). On the contrary, the behavior is different for O-rich clusters because they prefer dissociation into several pieces of SiO and SiO_2(BE_{II}). BE_I diminishes with m, indicating the increment in the number of (SiO) pieces, and BE_{II} grows with m, showing that the number SiO_2 pieces while the number of SiO pieces diminishes accordingly. This is additional evidence that SiO is more stable than SiO_2. Figure 8 shows that the best Si_6O_6 isomer is the less stable among these silicon-oxide systems, as we can see from the BE_I curve. This observation was also reported by Zang *et al.*[39]

We study some fragmentation pathways and the corresponding energies for the most stable structures of the series Si_6O_m ($m=1-11$) produced by MGAC/MSINDO/B3LYP methodology. Basically we choose those fragmentation channels formed by motifs that frequently appear in silicon-oxides studies (Si_2O_2, Si_3O_3, Si_3O_2, and Si_4O_4) and core silicon clusters Si_n ($n=2-5$). Furthermore, some fragmentation products contain SiO and SiO_2 molecules.

The energy for the fragmentation pathway $Si_6O_m \rightarrow Si_kO_l + Si_{6-k}O_{m-l}$ is defined as $FE = E(Si_kO_l) + E(Si_{6-k}O_{m-l}) - E(Si_6O_m)$ and the results are shown in Table II. The geometry of some of the fragmentation products, Si_kO_l and/or $Si_{6-k}O_{m-l}$, employed to evaluate the FEs were reported previously by Reber *et al.* and Lu *et al.*.[28,51] For Si_6O_{10} and Si_6O_{11} we propose alternative fragmentation pathways to be taken into account and our minimum is discussed in the following:

(1) Si_6O, Si_6O_2, and Si_6O_3: It is interesting to note that Si-rich clusters segregate in small Si cores, Si_5, Si_4 and Si_3 and SiO, Si_2O_2 and Si_3O_3 oxides, respectively. These channels agree with studies reported by Zang *et al.*[39] Wang *et al.*[43] also found that Si_nO has a tendency to segregate in Si_n+SiO. They also found recently[25] that some silicon monoxide clusters prefer to form *nearly* side polygonal Si clusters attached to monoxide silicon clusters. We found a similar behavior for Si-rich clusters, Si_6O, Si_6O_2, Si_6O_3, and some Si_6O_4, displayed in Fig. 1.

(2) Si_6O_4: In this case the most favorable fragmentation channel is $Si_6O_4 \rightarrow Si_3+Si_3O_4$, but its FE is only 0.04 eV smaller than the corresponding to the dissociation $Si_6O_4 \rightarrow Si_3O_3+Si_3O$.

(3) Si_6O_5 and Si_6O_6: Both cases contain the Si_3O_3 as one fragmentation product in the most favorable pathway. However, the energy fragmentation corresponding to the channel with a SiO fragment, $Si_6O_5 \rightarrow Si_5O_4+SiO$ and $Si_6O_6 \rightarrow Si_5O_5+SiO$, are higher by only 0.383 and 0.894 eV relative to the minimum FE, 2.177 and 0.729 eV, respectively. This observation is important because SiO is a very stable system.[25]

(4) Si_6O_7 to Si_6O_9: The most favorable pathway is $Si_6O_m \rightarrow SiO+Si_5O_{m-1}$. Si_6O_7 and Si_6O_8 show also a favorable dissociation into $Si_2O_2+Si_4O_5$ and $Si_2O_2+Si_4O_6$, respectively.

(5) Si_6O_{10} and Si_6O_{11}: In both cases, the new fragmentation pathways proposed here present energies higher than those reported by Zang *et al.*[39] However our most stable channels are those reported by Zang *et al.*[39]

Figure 9 shows a similar behavior for the LUMO-HOMO gap and the fragmentation energy against the number of oxygen atoms for the most stable isomer of the series Si_6O_m ($m=1-11$), except Si_6O_5. Clusters with high minimum fragmentation energy are particularly stable while large LUMO-HOMO gaps are indicative of chemical inertness.[44] Si_6O_6 is the less stable isomer for both criteria. The minimum energy fragmentation contains Si_2O_2, Si_3O_3, and SiO clusters, so these fragmentation products are considered to be

TABLE II. Fragmentation Energies (FE) and fragmentation channels for the most stable Si_6O_m (m=1–11) clusters found by the MGAC/MSINDO/B3LYP method.

Si_6O_m	$\rightarrow Si_kO_l$	$+Si_{6-k}O_{m-l}$	FE (eV)	Si_6O_m	$\rightarrow Si_kO_l$	$+Si_{6-k}O_{m-l}$	FE (eV)
Si_6O	Si_5 [a]	SiO	1.512	Si_6O_7	SiO	Si_5O_6 [b]	1.629
	Si_4 [a]	Si_2O [b]	2.793		Si_2O_2	Si_4O_5 [b]	2.088
	Si_3	Si_3O [b]	3.838		Si_3O_3	Si_3O_4 [b]	2.196
					Si_4O_4	Si_2O_3 [b]	4.149
Si_6O_2	Si_4 [a]	Si_2O_2	1.520		Si_3O_2	Si_3O_2	5.122
	Si_3	Si_3O_2	3.466		SiO_2	Si_5O_5 [b]	5.435
	Si_5 [a]	SiO_2 [b]	3.806				
				Si_6O_8	SiO	Si_5O_7 [b]	2.569
Si_6O_3	SiO	Si_5O_2	2.466		Si_2O_2	Si_4O_6 [b]	3.327
	Si_3	Si_3O_3	2.642		Si_3O_3	Si_3O_5 [b]	4.447
	Si_4 [a]	Si_2O_3 [b]	3.297		SiO_2	Si_5O_6 [b]	4.817
	Si_3O	Si_3O_2	4.223		Si_4O_4	Si_2O_4 [b]	6.593
					Si_3O_2	Si_3O_6 [b]	7.510
Si_6O_4	Si_3	Si_3O_4 [b]	2.403				
	Si_3O	Si_3O_3	2.443	Si_6O_9	SiO	Si_5O_8 [b]	3.124
	Si_3O_2	Si_3O_2	3.639		Si_2O_2	Si_4O_7 [b]	4.612
	Si_2	Si_4O_4	3.915		SiO_2 [b]	Si_5O_7 [b]	4.742
	Si_4 [a]	Si_2O_4 [b]	4.636		Si_4O_5 [b]	Si_2O_4 [b]	5.443
					Si_3O_3	Si_3O_6 [b]	5.821
Si_6O_5	Si_3O_3	Si_3O_2	2.177		Si_4O_4	Si_2O_5 [b]	10.423
	SiO	Si_5O_4 [b]	2.560				
	Si_4O_4	Si_2O [b]	2.774	Si_6O_{10}	SiO	Si_5O_9 [c]	3.606
	Si_2	Si_4O_5 [b]	2.992		SiO_2 [b]	Si_5O_8 [b]	4.475
	Si_3	Si_3O_5 [b]	3.867		Si_3O_5 [b]	Si_3O_5 [b]	4.713
	Si_4 [a]	Si_2O_5 [b]	8.693		Si_4O_6 [b]	Si_2O_4 [b]	4.845
					Si_3O_4 [b]	Si_3O_6 [b]	4.850
Si_6O_6	Si_3O_3	Si_3O_3	0.729				
	Si_2O_2	Si_4O_4	1.623	Si_6O_{11}	SiO	Si_5O_{10}	3.638
	SiO	Si_5O_5 [b]	1.646		Si_4O_7 [b]	Si_2O_4 [b]	4.816
	Si_3O_2	Si_3O_4 [b]	2.270		Si_5O_8 [b]	SiO_3 [b]	7.223
	SiO_2 [b]	Si_5O_4 [b]	4.975		Si_4O_6 [b]	Si_2O_5 [b]	7.360

[a]Geometries taken from Ref. 30.
[b]Geometries taken from Ref. 28.
[c]Geometries taken from Ref. 51.

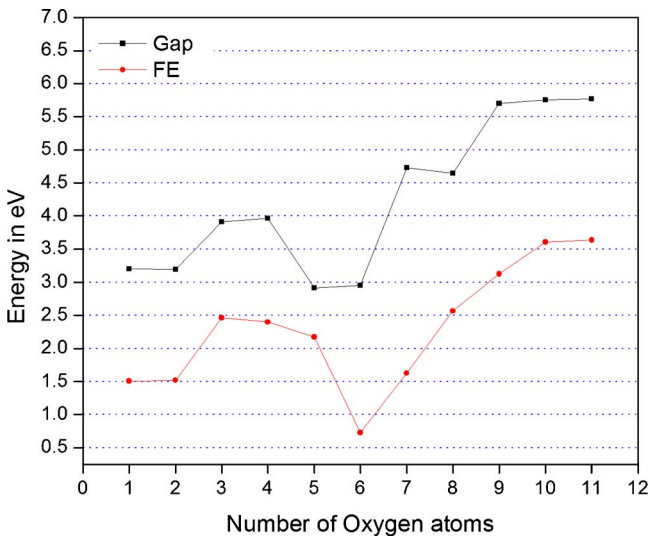

FIG. 9. (Color online) LUMO-HOMO gaps and minimum fragmentation energy FE for Si_6O_m(m=1–11) clusters.

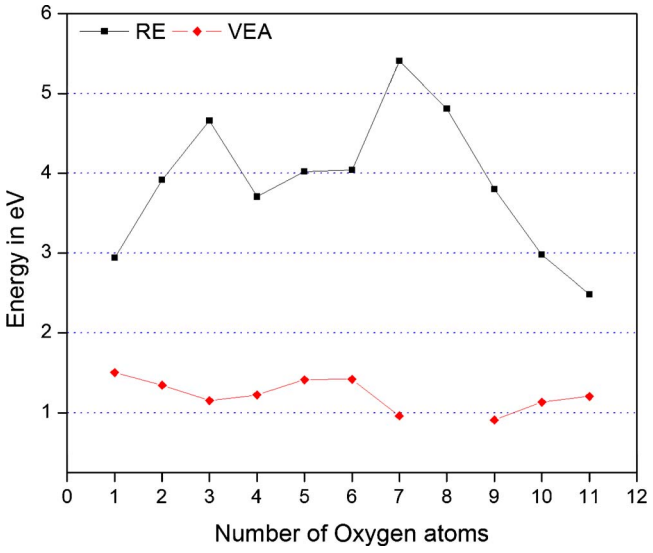

FIG. 10. (Color online) Energy required to remove one oxygen RE and the VEA for Si_6O_m (m=1–11) clusters.

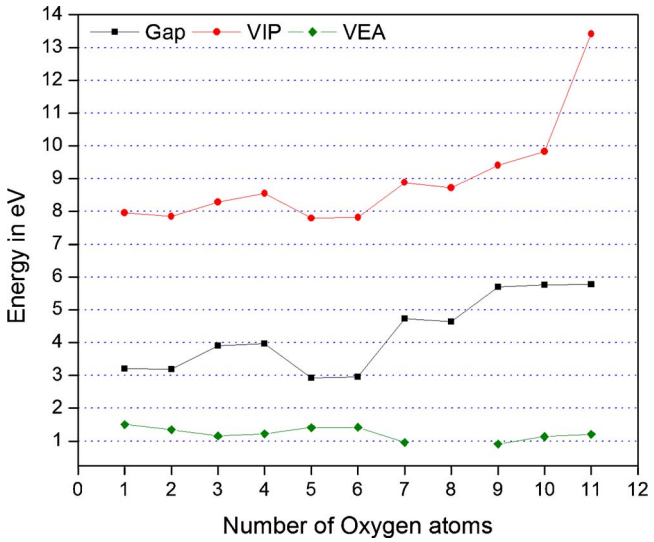

FIG. 11. (Color online) LUMO-HOMO gap, the vertical ionization potential VIP and the VEA for Si_6O_m ($m=1-11$) clusters.

relatively stable clusters. These results are in good agreement with the experimental data reported by Rebert *et al.*[28]

We define RE as the energy required to remove one oxygen atom, that is $RE=E(Si_6O_{m-1})+\frac{1}{2}E(O_2)-E(Si_6O_m)$. RE is either the energy required to remove one oxygen atom from Si_6O_m or the incremental energy on adding one oxygen atom to the Si_6O_{m-1} system. Because of that, the peaks observed in Fig. 10 are an indication of the cluster stability. Si_6O_3 for the Si-rich clusters and Si_6O_7 for the O-rich clusters are the most stable systems. For these systems the vertical electron affinity (VEA) reaches its corresponding minima, plotted also in Fig. 10, against the number of oxygen atoms. These peaks have a correspondence with the minimum ones presented in the VEAs.

The vertical ionization potential (VIP), VEA, and LUMO-HOMO gap for the most stable Si_6O_m ($m=1-11$) isomers are plotted in Fig. 11 as a function of m. The GAP is between 3.19 and 3.96 eV for Si-rich systems ($Si_6O_m, m=1-4$) and 2.92 and 5.77 eV for O-rich systems, and the VIPs are approximately 8–10 eV for Si_6O_{1-10} and greater (14 eV) for the Si_6O_{11} cluster. VEAs vary from 0.9 to 1.5 eV. These results indicate that Si_6O_m structures obtained from the MGAC/MSINDO/B3LYP production are stable against losing or adding electrons. We conclude that Si_6O_3 and Si_6O_4 are the most stable isomers among Si-rich clusters and Si_6O_{9-11} is the most stable among O-rich clusters. Figure 11 shows a similar small LUMO-HOMO gap for Si_6O_5 and Si_6O_6, the clusters with O/Si close to one.

Si_6O_8 was not included on Figs. 10 and 11 because the B3LYP-VEA is negative for our convention. So we evaluated the affinity for this system, allowing the geometrical relaxation (adiabatic electron affinity, AEA). B3LYP did not find an appropriate state for the anion. Instead, the B3PWN functional gave the right sign (AEA=1.027 eV) (Ref. 45) indicating that B3LYP cannot represent properly the Si_6O_8 anion.

We report in Table III principal modes for the most stable Si_6O_m ($m=1-11$) clusters produced in this work. They are identified, in the same table, with the vibration frequencies of the corresponding fragmentation products measured by Anderson and Ogden.[13] It offers an additional evidence of the presence of 2MR and 3MR fragmentation products.

Figure 12 shows the HOMO and the LUMO for the best isomer of each system, which presents 2MR, 3MR, or 4MR motif. It is interesting to highlight that the HOMOs and LUMOs are located preferably in those regions of the cluster where those motifs are not present, i.e., outside of the motifs. This is the case of the systems Si_6O_9, Si_6O_{10}, and Si_6O_{11}.

TABLE III. Vibration frequencies for Si_6O_m ($m=1-11$) clusters and some of their fragmentation products. We report the frequencies for principal modes of the most stable isomer of each cluster.

	Vibration frequencies				Vibration frequencies		
Si_6O_m [a]	Principal modes		Fragmentation product[b]	Si_6O_m [a]	Principal modes		Fragmentation product[b]
Si_6O	851.5				1018.1	1008.4[a]	(SiO_2)
	466.7	460.0[c]	(Si_6)	Si_6O_8	1038.0		
Si_6O_2	903.1	1008.4[a]	(SiO_2)		1079.0		
Si_6O_3	957.7	957.6[a]			1007.7	691.1[a]	(SiO_2)
	977.3	972.6[d]	(Si_3O_3)	Si_6O_9	1100.9	957.6[a]	
Si_6O_4	794.7	766.6[a]				972.6[d]	(Si_3O_3)
		766.3[d]	(Si_2O_2)		1101.6		
	1012.7	1008.4[a]	(SiO_2)		870.2	801.3[a]	
Si_6O_5	1010.2	1008.4[a]	(SiO_2)			804.7[d]	(Si_2O_2)
	942.5	954.8[a]		Si_6O_{10}	935.3	1008.4[a]	(SiO_2)
	975.9	957.6[a]			776.5	766.6[a]	
Si_6O_6		972.6[d]	(Si_3O_3)			766.3[d]	
Si_6O_7	935.6	1008.4[a]	(SiO_2)		801.6	801.3[a]	
	1000.4					804.7[d]	(Si_2O_2)
				Si_6O_{11}	932.8	1008.4	(SiO_2)

[a]This work.
[b]Indicated in $Si_6O_m \rightarrow Si_kO_l + Si_{6-k}O_{m-l}$.
[c]Geometry taken from Ref. 30.
[d]Vibration frequencies from the mass spectra reported in Ref. 13 for the fragmentation products.

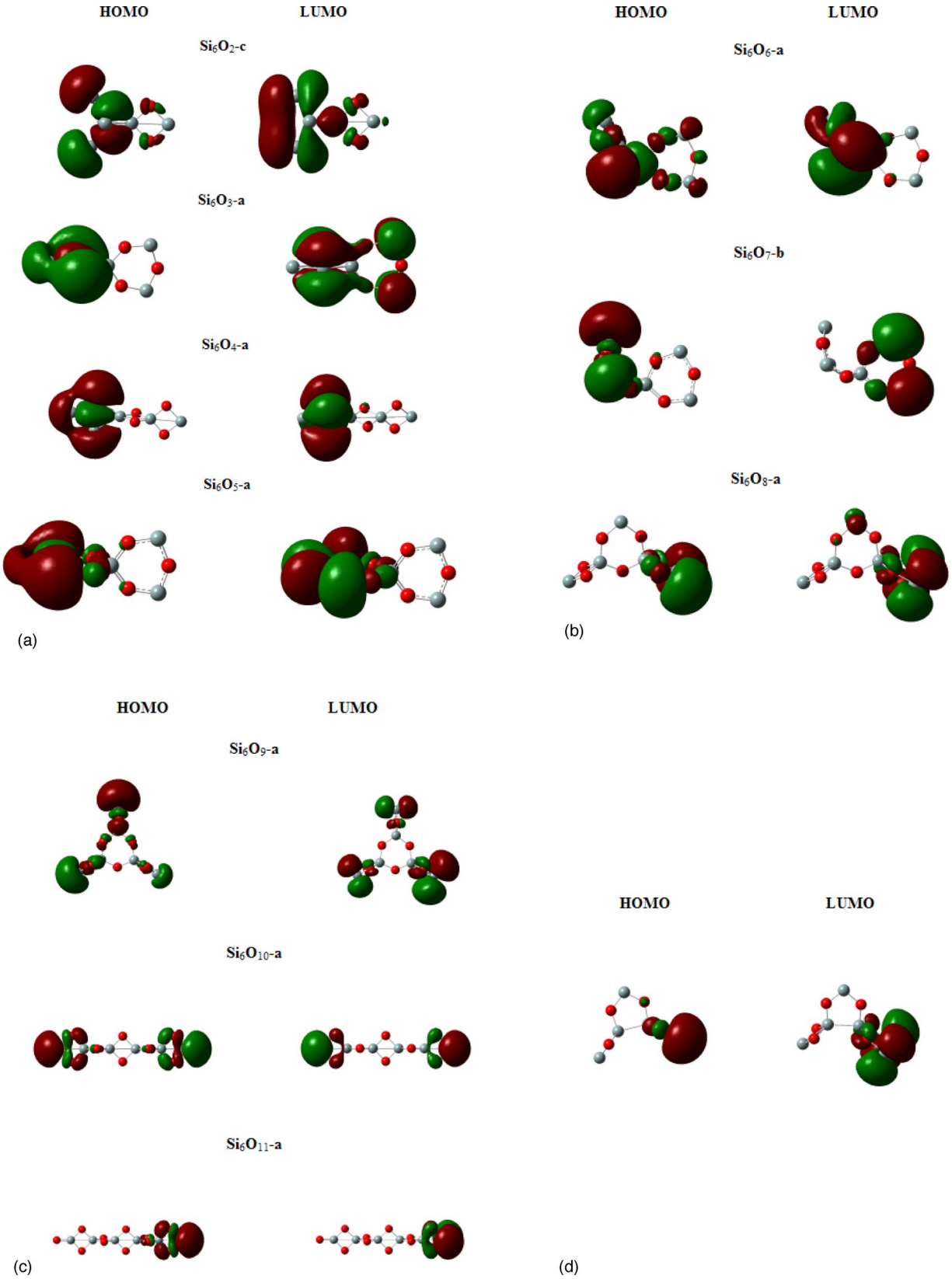

FIG. 12. (Color online) (a–c) HOMOs and LUMOs of the most stable Si_6O_m ($m=2-11$) clusters which present 2MR, 3MR, or 4MR motifs. The isovalue of the contour map is 0.02. (d) HOMO and LUMO of the Si_6O_7-*c* cluster which present Si_3O_2 motifs. The isovalue of the contour map is 0.02.

This behavior was mentioned by Wang *et al.* in the Ref. 25, the HOMOs and LUMOs are mostly located at pure silicon clusters.

Static dipole polarizability is one of the fundamental properties of any atomic or molecular system. It has been extensively studied with theoretical as well as with experimental methods. In the field of atomic clusters, dipole polarizability has become one of the most important quantities to

TABLE IV. For each value of m (number of oxygen atoms) we report $\boldsymbol{\alpha}_{\text{best}}$, the polarizability of the most stable isomer, and $\boldsymbol{\sigma}$ (vertical bars in Fig. 13), the dispersion of the polarizabilities of the other isomers around $\boldsymbol{\alpha}_{\text{best}}$. Also, we report the polarizability anisotropy $\Delta\alpha$ for silicon oxides. All data are expressed in a.u.

System	α_{best}	σ	α_{best}/m	$\Delta\alpha$	$\Delta\alpha$/m
Si_6O	182	8	182	3183	3183
Si_6O_2	179	13	89	2835	1417
Si_6O_3	186	6	62	13 878	4626
Si_6O_4	174	12	44	19 729	4932
Si_6O_5	178	3	36	6234	1247
Si_6O_6	169	6	28	1492	249
Si_6O_7	151	7	22	348	50
Si_6O_8	152	1	19	1409	176
Si_6O_9	141	4	16	2641	293
Si_6O_{10}	136	1	14	10 892	1089
Si_6O_{11}	132	3	12	11 437	1040

guess the clusters geometry.[46] The dipole polarizability indirectly provides a measure of the extent of distortion in the electron density and hence the response of the system under the effect of an external static electric field. It is sensitive to the nature of the bonding and the geometrical structure of the system. Several authors studied the relation between cluster shape and polarizability per atom.[47,48]

In general, the static response properties of a molecule can be defined by expanding the field-dependent energy W(E) as a series in the components of a uniform electric field E,

$$W(E) = W_o + \mu_i E_i + \tfrac{1}{2}\alpha_{ij}E_iE_j + \ldots \quad (i,j = x,y,z), \tag{8}$$

where W_o is the energy of the system in absence of electric field, μ_i is the dipole moment, and α_{ij} is the ij component of the polarizability tensor (repeated Greek subscripts imply summation over Cartesian coordinates, x, y, and z).

$$\alpha_{ij} = \left(\frac{d^2W}{dE_i dE_j}\right)_{E=0}. \tag{9}$$

In this work, we computed the static dipole polarizabilities for ground state structures. The calculations have been carried out in the framework of DFT implemented in the GAUSSIAN code,[42] using B3LYP exchange correlation functional and 6-311G(2d) basis set. The mean polarizability α and the polarizability anisotropy $\Delta\alpha$ for silicon oxides were calculated from equations

$$\alpha = \tfrac{1}{3}(\alpha_{xx} + \alpha_{yy} + \alpha_{zz}) \tag{10}$$

and

$$\Delta\alpha = \frac{1}{2}\sum_{i,j=x,y,z}(\alpha_{ii} - \alpha_{jj})^2. \tag{11}$$

The polarization anisotropy $\boldsymbol{\Delta\alpha}$ seems to be the convenient quantity to evaluate how much the cluster shape differs from one spherical molecule.

The results for α and $\boldsymbol{\Delta\alpha}$ are reported in Table IV and depicted in Figs. 13 and 14. For each value of **m** (number of oxygen atoms) we report $\boldsymbol{\alpha}_{\textbf{best}}$, the polarizability of the most stable isomer, and $\boldsymbol{\sigma}$ (vertical bars in Fig. 13), the dispersion of the polarizabilities for the other Si_6O_m isomers around $\boldsymbol{\alpha}_{\textbf{best}}$, defined as

$$\sigma_m = \frac{\sum_{i=1}^{N_m}(\alpha_{im} - \alpha_{bestm})^2}{N_m}, \tag{12}$$

where N_m is the number of isomers for each Si_6O_m series.

We can see that the $\boldsymbol{\alpha}$/**m** values present an asymptotic tendency as a function of the number of oxygen atoms **m**, different from the behavior of the homonuclear silicon clusters.[30,35] for which the quantity $\boldsymbol{\alpha}$/**atom** is approximately constant. This behavior is curious and very interesting. Clusters with large LUMO-HOMO gaps are indicative of chemical inertness[44] and the dipole polarizability indirectly provides a measure of the extent of distortion in the electron density, so clusters with large LUMO-HOMO gaps will have low polarizability.[49,50] Our hypothesis is that the oxygen electronegativity plays an important role in the tendency shown in Fig. 13. Oxygen pulls the electrons and successive oxidation might contribute to increase the "*system electrone-*

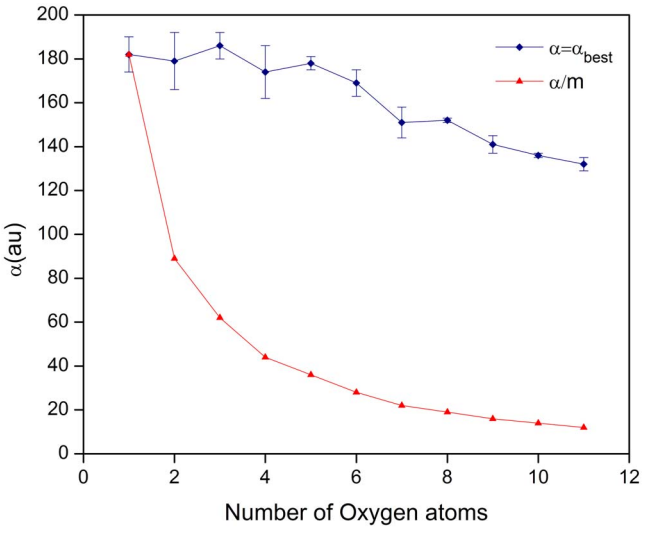

FIG. 13. (Color online) The polarizability of the most stable isomer, $\boldsymbol{\alpha}_{\textbf{best}}$ (♦) and α/m (▲), as a function of m, the number of oxygen atoms. The vertical bars in $\boldsymbol{\sigma}$ indicate the dispersion of the other Si_6O_m isomers around $\boldsymbol{\alpha}_{\textbf{best}}$, as defined in Eq. (12).

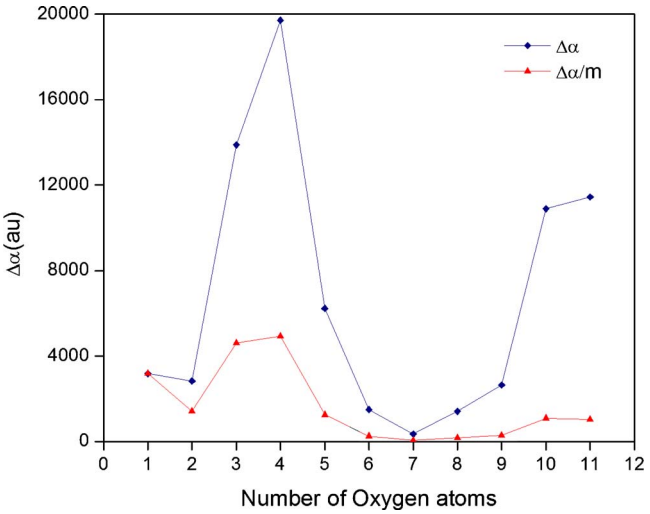

FIG. 14. (Color online) The polarization anisotropy, $\Delta\alpha$ (♦) and $\Delta\alpha/m$ (▲), as a function of m, the number of oxygen atoms.

gativity" causing the polarizabilities to decrease. To our knowledge, there are neither calculations nor experimental data of silicon oxides polarizabilities in the literature. Present evaluations show that this topic needs of further studies to provide additional explanations for the very interesting observed tendency. Note that $\boldsymbol{\Delta\alpha}$ in Fig. 14, which is positive by definition, is in total correspondence with the cluster shape, oblate, or prolate, illustrated by the inertia momentum depicted in Fig. 7.

IV. CONCLUSIONS

We have shown that our results agree well with previously reported structures and we found new ones. The system prefers to form 2MR and 3MR motifs. This characteristic is important in the geometric determination of Si_6O_{9-11} clusters, which present only combinations of 2MR and 3MR.

The behavior of BE per atom calculated in this work reproduces the features observed by other authors. For $m<6$, the dissociation proceeds to SiO, while for $6\leq m\leq 12$ the preferred decay channel is $(m-6)SiO_2$ plus $(12-m)SiO$ molecules. For $m\geq 12$, finally, the favored channel is SiO_2 plus oxygen. The minimum energy fragmentation pathways contain Si_2O_2, Si_3O_3, and SiO clusters so these fragmentation products are considered to be relatively stable clusters.

We did not find experimental data or theoretical evaluations of Si_6O_m polarizabilities in the literature to compare with our calculations, but the behavior of the polarizability against oxidation is very interesting and needs further investigation. However, we note that $\boldsymbol{\Delta\alpha}$ is in total correspondence with the cluster shape compact, oblate, or prolate.

The behavior of the LUMO-HOMO gap shows that it is more difficult to ionize Si-rich clusters than O-rich clusters. Si_6O_3 and Si_6O_4 are the most stable isomers among Si-rich clusters and Si_6O_{9-11} is the most stable among O-rich clusters. Finally we observed that HOMOs and LUMOs are located preferably in those regions of the cluster where those motifs are not present, i.e., outside of the motifs.

ACKNOWLEDGMENTS

Financial support to this work from the University of Buenos Aires and from the Argentinean CONICET is gratefully acknowledged. Generous resources allocations at the Center for High Performance Computing (CHPC-Utah University) are also acknowledged.

[1] D. L. Helms, *Elements of Physical Geology* (Ronald, New York, 1969).
[2] G. W. Morey, *The Properties of Glass* (Reinhold, New York, 1954).
[3] W. Wang, B. Gu, L. Liang, and W. Hamilton, J. Phys. Chem. B **107**, 3400 (2003).
[4] J. L. Gole and Z. L. Wang, Nano Lett. **1**, 449 (2001).
[5] E. Desurvire, Phys. Today **47**, 20 (1994).
[6] L. Brus, J. Phys. Chem. **98**, 3575 (1994).
[7] S. Li, S. J. Silvers, and M. S. El-Shall, J. Phys. Chem. B **101**, 1794 (1997).
[8] I. S. Altman, D. Lee, J. D. Chung, J. Song, and M. Choi, Phys. Rev. B **63**, 161402(R) (2001).
[9] Y. D. Glinka, S. H. Lin, Y. T. Lin, and Y. T. Chen, Phys. Rev. B **62**, 4733 (2000).
[10] S. T. Bromley, Nano Lett. **4**, 1427 (2004).
[11] H. van Beckkum, P. A. Jacobs, E. M. Flanigen, and J. C. Jansen, *Introduction to Zeolite Science and Practice, Studies in Surface Science and Catalysis* (Elsevier, Amsterdam, 2001), Vol. 137.
[12] N. Wang, Y. H. Tang, Y. F. Zhang, C. S. Lee, and S. T. Lee, Phys. Rev. B **58**, 16024(R) (1998).
[13] J. S. Anderson and J. S. Ogden, J. Chem. Phys. **51**, 4189 (1969).
[14] L. S. Wang, J. B. Nicholas, M. Dupuis, H. Wu, and S. D. Colson, Phys. Rev. Lett. **78**, 4450 (1997).
[15] L. S. Wang, S. R. Desai, H. Wu, and J. B. Nicholas, Z. Phys. D **40**, 36 (1997).
[16] L. S. Wang, H. Wu, S. R. Desai, J. Fan, and S. D. Colson, J. Phys. Chem. **100**, 8697 (1996).
[17] J. R. Chelikowsky, Phys. Rev. B **57**, 3333 (1998).
[18] L. C. Snyder and K. J. Raghavachari, J. Chem. Phys. **80**, 5076 (1984).
[19] R. Q. Zhang, T. S. Chu, H. F. Cheung, N. Wang, and S. T. Lee, Phys. Rev. B **64**, 113304 (2001).
[20] J. Song and M. Choi, Phys. Rev. B **65**, 241302(R) (2002).
[21] S. K. Nayak, B. K. Rao, and P. Jena, J. Chem. Phys. **109**, 1245 (1998).
[22] T. S. Chu, R. Q. Zhang, and H. F. Cheung, J. Chem. Phys. **105**, 1705 (2001).
[23] A. D. Becke, J. Chem. Phys. **98**, 5648 (1993).
[24] D. Zhang, M. Zhao, and R. Q. Zhang, J. Phys. Chem. B **108**, 18451 (2004).
[25] H. Wang, J. Sun, W. C. Lu, Z. S. Li, C. C. Sun, C. Z. Wang, K. M. Ho, J. Phys. Chem. C **112**, 7097 (2008).
[26] Y. F. Zhang, Y. H. Tang, N. Wang, D. P. Yu, C. S. Lee, I. Bello, and S. T. Lee, Appl. Phys. Lett. **72**, 1835 (1998).
[27] R. Q. Zhang, Y. Lifshits, and S. T. Lee, Adv. Mater. (Weinheim, Ger.) **15**, 635 (2003).
[28] A. C. Reber, S. Paranthaman, P. A. Clayborne, S. N. Khanna, and A. Welford Castleman, Jr., ACS Nano **2**, 1729 (2008).
[29] V. E. Bazterra, M. B. Ferraro, and J. C. Facelli, J. Chem. Phys. **116**, 5984 (2002).
[30] V. E. Bazterra, O. Oña, M. C. Caputo, M. B. Ferraro, P. Fuentealba, and J. C. Facelli, Phys. Rev. A **69**, 053202 (2004).
[31] V. E. Bazterra, M. Cuma, M. B. Ferraro, and J. C. Facelli, J. Parallel Distrib. Comput. **65**, 48 (2005).
[32] D. J. Wales and H. A. Scheraga, Science **285**, 1368 (1999).
[33] D. J. Wales and M. P. Hodges, Chem. Phys. Lett. **286**, 65 (1998).
[34] S. Kirkpatrick, C. D. Gellatt, and M. Vecchi, Science **220**, 671 (1983).
[35] O. Oña, V. E. Bazterra, M. C. Caputo, J. C. Facelli, P. Fuentealba, and M. B. Ferraro, Phys. Rev. A **73**, 053203 (2006).
[36] B. Ahlswede and K. Jug, J. Comput. Chem. **20**, 563 (1999).
[37] B. Ahlswede and K. Jug, J. Comput. Chem. **20**, 572 (1999).
[38] T. Bredow, G. Geudtner, and K. Jug, J. Comput. Chem. **22**, 861 (2001).
[39] Q. J. Zang, Z. M. Su, W. C. Lu, C. Z. Wang, and K. M. Ho, J. Phys. Chem. A **110**, 8151 (2006).
[40] R. Q. Zhang and W. J. Fan, J. Cluster Sci. **17**, 541 (2006).
[41] R. L. Johnston and C. Roberts, in *Soft Computing Approaches in Chemistry*, edited by H. M. Cartwright and M. Sztandera (Springer-Verlag, Heildberg, 2003), Vol. 120, p.161.

[42] M. J. Frisch, G. W. Trucks, H. B. Schlegel *et al.*, GAUSSIAN, Gaussian, Inc, Pittsburgh PA, 1998.
[43] H. Wang, W. C. Lu, C. C. Sun, C. Z. Wang, and K. M. Ho, Phys. Chem. Chem. Phys. **7**, 3811 (2005).
[44] A. Welford Castleman, Jr., S. N. Khanna, A. Sen, A. C. Reber, M. Qian, K. M. Davis, S. J. Peppernick, A. Ugrinov, and M. D. Merritt, Nano Lett. **7**, 2734 (2007).
[45] The VEA and adiabatic (AEA), calculated with different methods of DFT are: 0.958 eV (VEA), 1.089 eV (AEA) for Si_6O_7 and 0.907 eV (VEA), 0.971 eV (AEA) for Si_6O_9, employing the B3LYP functional. They are instead, 1.024 eV (VEA), 1.184 eV (AEA) for Si_6O_7 and 0.951 eV (VEA), 1.011 eV (AEA) for Si_6O_9, employing the B3PWN functional. Therefore, Si_6O_8 may be considered as a particular case for this property and the use of B3LYP o B3PWN is similar for the other systems considered in this manuscript.
[46] W. A. de Heer, Rev. Mod. Phys. **65**, 661 (1993).
[47] K. A. Jackson, M. Yang, I. Chaudhuri, and Th. Frauenheim, Phys. Rev. A **71**, 033205 (2005).
[48] K. Deng, J. Yang, and C. T. Chan, Phys. Rev. A **61**, 025201 (2000).
[49] R. G. Pearson, J. Chem. Educ. **45**, 981 (1968).
[50] R. G. Parr and Z. Zhou, Acc. Chem. Res. **26**, 256 (1993).
[51] W. C. Lu, C. Z. Wang, V. Nguyen, M. W. Schmid, M. S. Gordon, and K. M. Ho, J. Phys. Chem. A **107**, 6936 (2003).